SUPPLEMENTARY INFORMATION

On-surface synthesis of metal-organic frameworks:
the critical role of the reaction conditions

Nerea Ruiz del Árbol[a,1], Carlos Sánchez-Sánchez[a,1], José I. Martínez[a], Luis Rodríguez[a],
David Serrate[b,c], Alberto Verdini[c], Luca Floreano[c], Peter Jacobson[d,2],
Leonhard Grill[d], José A. Martín-Gago[a], María F. López[a*]

[a] Instituto de Ciencia de Materiales de Madrid (ICMM), CSIC,
Sor Juana Inés de la Cruz 3, 28049 Madrid, Spain

[b] Instituto de Nanociencia y Materiales de Aragón (INMA), CSIC-UNIZAR,
50009 Zaragoza, Spain

[c] Laboratorio de Microscopias Avanzadas (LMA), Universidad de Zaragoza,
50018 Zaragoza, Spain

[c] CNR-IOM, Laboratorio TASC, Basovizza SS-14, Km 163.5, I-34149 Trieste, Italy

[d] Department of Physical Chemistry, University of Graz, Heinrichstrasse 28,
8010 Graz, Austria

CONTENTS

[1] Nerea Ruiz del Árbol and Carlos Sánchez-Sánchez contributed equally to this work as first authors.
[2] Current affiliation: School of Mathematics and Physics, The University of Queensland, Brisbane, Queensland 4072, Australia

1. Experimental methods

All the experiments were performed in UHV systems with a base pressure of 1 x 10^{-10} mbar. A Cu(111) surface was cleaned by sputtering-annealing cycles until the surface was free of contaminants, as confirmed by LEED and STM. The p-AP molecules (Sigma-Aldrich, 99% purity) were deposited at room temperature from a glass vessel using their vapour pressure under UHV conditions, reaching a base pressure during evaporation in the 10^{-9} mbar range.

For the formation of the molecular network, two different experimental strategies were applied, as well as two distinct systems. For protocol **1**, in which the p-AP molecules were deposited on the Cu(111) sample at RT and then annealed at high temperature, a SPECS Joule Thompson STM was used. For protocol **2**, in which the p-AP molecules were directly deposited on an annealed Cu(111) sample, a Createc LT-STM/AFM was used. After preparation, the sample was cooled and transferred to the microscope. All STM images were recorded at a temperature of about 5 K.

The x-ray photoelectron spectroscopy (XPS) measurements were performed at the ALOISA beamline of the Elettra synchrotron radiation facility in Trieste (Italy). The high-resolution XPS spectra were recorded at the O 1s, N 1s and C 1s regions with a hemispherical analyzer oriented along the linerally polarized electric field while keeping the sample at a grazing incidence of 4.0˚ (close to normal emission and *p*-polarization). The electron spectrometer is a home-made hemispherical analyzer equipped with a high dynamic range (2 Mhz) 2D delay-line detector. All spectra were acquired at RT. The photon energies used for the XPS measurement of the O1s, N1s and C1s spectra were 650 eV, 500 eV and 400 eV, with a corresponding overall energy resolution of 260, 170 and 150 meV, respectively. The binding energy scale was calibrated to the Fermi level. We verified that no significant radiation damage took place on the timescale of the spectroscopy measurements by comparison of photoemission spectra measured on irradiated and fresh sample areas.

2. STM images

For the formation of the two different networks, the topological Kagome and the canonical honeycomb lattice, we have used two different experimental conditions. One the one hand, we have

deposited the molecules on a clean Cu(111) surface at RT with subsequent post-annealing to higher temperatures. This experimental process gives rise to the Kagome network. On the other hand, the experimental process consisting on dosing the molecules directly on the hot Cu(111) surface originates the honeycomb lattice.

Figure S1a shows an STM image of p-AP molecules adsorbed on Cu(111) after their deposition at RT. Although the saturation of the surface was not complete, it was quite close, with p-AP molecules covering almost the entire surface. Upon annealing the sample at around 500 K, the p-AP molecules arrange to form a network, as can be observed in Figure S1b. The STM image of this figure shows the formation of islands of p-AP molecules arranged forming a network, whose molecular order and conformation can be better appreciated in Figure 1a of the main manuscript. On the other hand, there are some isolated groups of molecules dispersed along the surface that are not forming a metal-organic framework (some of them highlighted with white closed curves in Figure S1b). We propose that in these clusters, N is not completely dehydrogenated, but in the form of -NH, accounting for the small Ph-NH component in the N-1s XPS spectra (green spectrum in N1s region of Figure 2).
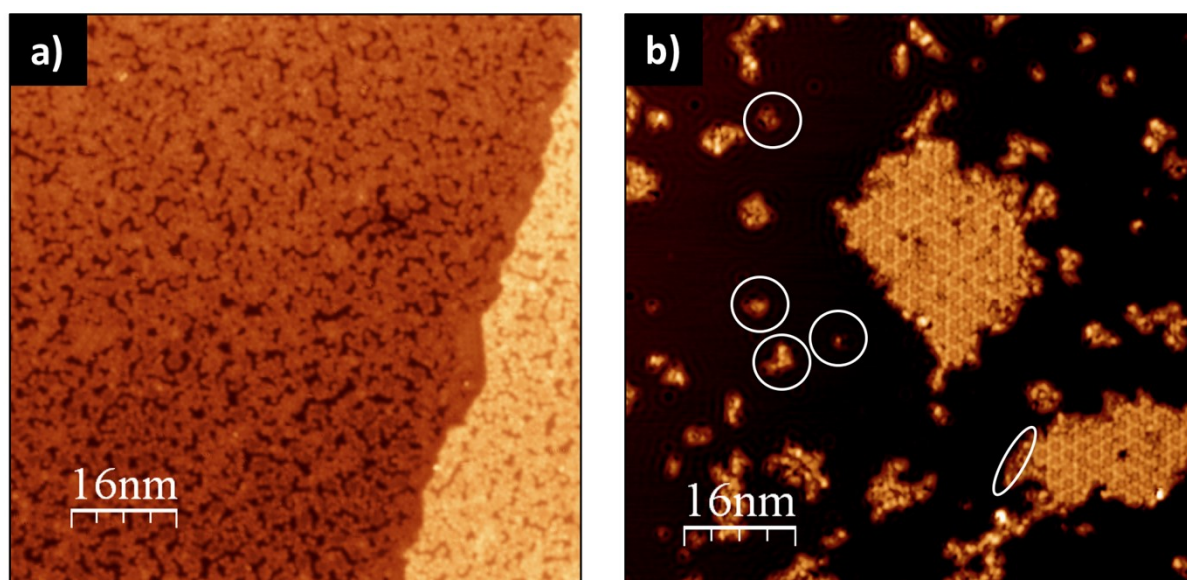

Figure S1. *a) LT-STM image of p-AP after deposition on the Cu(111) surface at RT ($V_{bias}= 1$ V, $I_t= 35$ pA). b) LT-STM image of p-AP on Cu(111) after annealing at ~ 500 K ($V_{bias}= 1$ V, $I_t= 31$ pA).*

Figure S2 shows two STM images of p-AP molecules deposited on Cu(111) at ~ 500 K. In both images, the presence of different network islands protruding from the step edges can be appreciated. Similarly to the previous case, isolated groups of molecules not forming metal-organic frameworks as well as molecules at the borders of the frameworks islands (some of them highlighted in white in Figure S2b) would be responsible of the Ph-NH component in the N-1s XPS spectra (blue spectrum in N1s region of Figure 2).
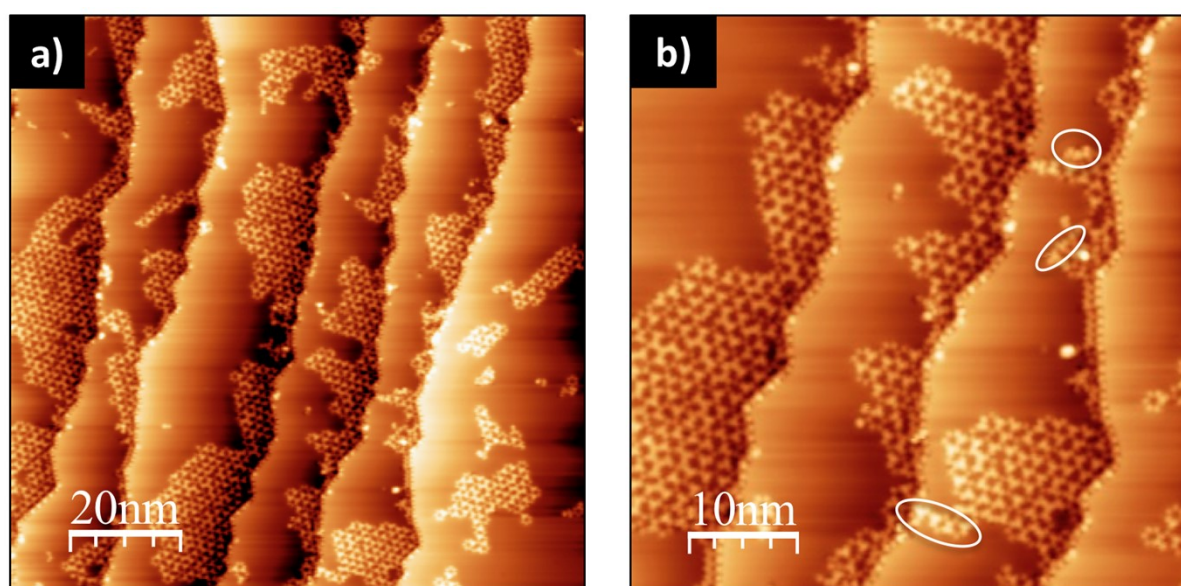

Figure S2. *STM images of p-AP deposited on the Cu(111) surface at ~ 500 K (V_{bias}= -1.1 V, I_t=0.24 nA).*

3. XPS measurements

Figure S3a shows the O1s XPS spectra of p-AP deposited on the Cu(111) at RT and after step-by step-annealing to different temperatures, 330 K and 510 K. After deposition of p-AP on the surface at RT, the O1s spectrum exhibits two components located at binding energies (BE) of 530.7 eV and 532.8 eV, respectively. The main subspectrum corresponds to either a ketone or a phenoxy group, revealing that the dehydrogenation of the alcohol group of p-AP already starts as soon as the molecules reach the Cu(111) surface at RT [1]. The small subspectrum at 532.8 eV corresponds to the alcohol group, i.e., to molecules which did not undergo the dehydrogenation process of this terminal group [1]. Upon heat

treatment, already at 330 K this small component disappears, indicating the complete dehydrogenation of all alcohol groups. In the spectrum obtained after annealing at 510 K, a new peak at a BE of 533.6 eV is detected. This emission can be attributed to O-containing organic species that emerge from the initial fragmentation of p-AP at defects [2].
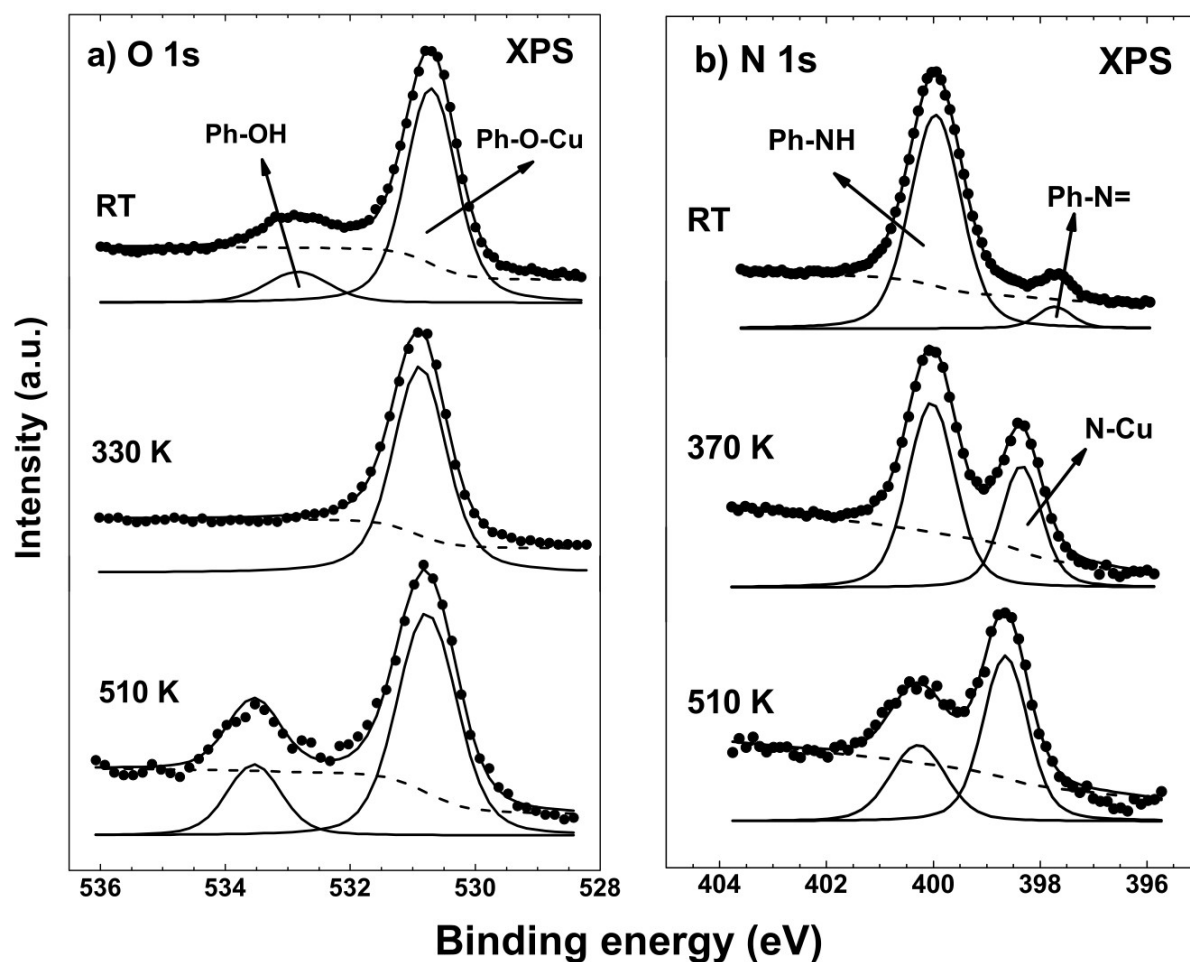

Figure S3. *a) O1s and b) N1s XPS spectra of p-AP deposited on the Cu(111) at RT and subsequent step-by step-annealing to different temperatures.*

Figure S3b shows the N1s spectra of p-AP deposited on the Cu(111) at RT and after step-by step-annealing to different temperatures, 370 K and 510 K. After deposition of p-AP on the surface at RT, the N1s spectrum exhibits two components located at BE of 399.9 eV and 397.5 eV, respectively. The main subspectrum, at 399.9 eV, originates from the partial dehydrogenation of the amine group upon molecular adsorption (-NH), while the signal at 397.5 eV corresponds to an iminic (-N=) component,

i.e., to molecules which undergo complete dehydrogenation of the amine group [3]. This small component disappears at 370 K, where an intense emission arises at 398.7 eV. This subspectrum, which further increases until becoming the main peak when annealing at 510 K, originates from the metalation reaction of the amine group of p-PA molecules with Cu adatom of the surface [3,4], and corresponds, therefore, to the formation of the metal-organic network. In the spectrum obtained after annealing at 510 K, the peak corresponding to -NH, at 399.9 eV, decreases becoming a small component. As the first principle calculations reveal that the amine groups in the metal-organic networks are fully dehydrogenated, this small emission is associated either to isolated groups of molecules, which are not part of any metal-organic network, or to molecules belonging to a network but located at the network edges, which could have -NH ending groups (see regions highlighted in white in Figures S1b and S2b).

4. Theoretical framework, computational details and modelling of the interfacial networks

On the basis of the XPS and STM experimental evidence, a large battery of Density Functional Theory (DFT) calculations, as implemented in the plane-wave QUANTUM ESPRESSO simulation package [5], has been carried out for the structural optimization of the two different interfacial networks, as well as for the elucidation of their electronic structure properties. One-electron wave-functions were expanded in a plane-waves basis with energy cutoffs of 500 and 600 eV for the kinetic energy and the electronic density, respectively. Electronic exchange and correlation have been computed within the revised generalized gradient corrected approximation PBESol [6,7]. Kresse-Joubert projector augmented wave pseudopotentials [8] have been adopted to model the ion-electron interaction for all the involved atoms (H, C, N, O and Cu). Brillouin zones have been sampled by using optimal ($2\times2\times1$) Monkhorst-Pack grids [9]. A perturbative van der Waals (vdW) formalism, with an empirical vdW R-6 correction, was used to add dispersive forces to conventional density functionals (DFT+D3)[10]. Atomic relaxations were carried out using a conjugate gradient minimization scheme until the maximum force on any atom was lower than 0.02 eV $Å^{-1}$. The Fermi level was smeared out using the Methfessel–Paxton approach [11] with a Gaussian width of 0.01 eV, and all energies were extrapolated to T=0 K. Self-consistency in the electron density was converged to a precision in the total energy better than 10^{-6} eV.
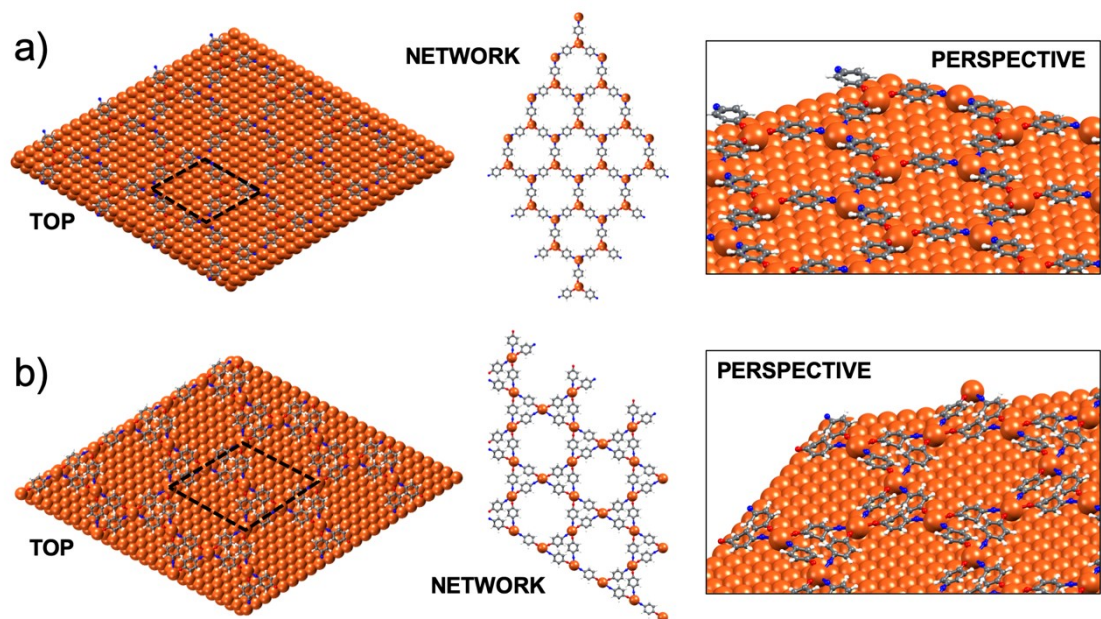
Figure S4. Different pictorial views for the two optimized interfacial networks: top view, view of the networks with the substrate removed for a better visualization, and perspective view (from left to right).

To construct all the interfacial models in the search of the ground-state, used as trial system geometries in the calculations, we have considered: i) a slab of 4 physical Cu(111) layers, with a minimum distance of ~25 Å of vacuum between neighboring cells along the axis perpendicular to the surface, and ii) full-periodic boundary conditions representing an infinite Cu(111) surface. For the structural optimization calculations (with the p-AP molecules on the surface) the 2 bottommost Cu(111) physical layers were kept fixed. Network periodicity along selected directions obtained from the experimental STM profiles have guided us to construct perfectly commensurate starting-point interfacial structures, which, after relaxation, have yielded ground-state configurations (see Figure S4) for each on-surface network with hexagonal symmetry with lattice parameters of 1.42 and 2.07 nm, very close to the experimental values of 1.5± 0.05 and 2.11± 0.06 nm, respectively. In the Kagome lattice, the coordinating Cu adatoms are located at an average distance of approximately 0.24 nm over the surface, whilst the centre of mass of the molecules are slightly higher, at an average distance of around 0.31 nm. In the honeycomb lattice, the coordinating Cu adatoms are located at an average distance above the surface of approximately 0.23 nm, whilst the molecules are almost flat, although slightly bent, at an average distance of their C-rings

of around 0.32 nm. The atomic density of the honeycomb and Kagome lattices is 18.03 and 20.97 atoms/nm^2, respectively.

For the STM-imaging simulations, a local-orbital formulation of DFT was also used, as implemented in the FIREBALL code (see [12] and references therein), in which self-consistency is implemented on the orbital occupation numbers [12,13] obtained using the orthonormal Löwdin orbitals [11]. Tunneling currents for the STM images have been computed by using the Keldysh-Green function formalism for the two ground-state networks obtained from the previous geometrical optimization calculations, together with the first-principles tight-binding Hamiltonian obtained from the FIREBALL code (as explained in full detail elsewhere [11,14]). All computed theoretical STM images have been obtained at constant-current scanning conditions in order to mimic the experimental procedure (in this case Itunnel = 0.1 nA and Vs = +1.0 V).

5. Supplementary references

[1] R. Zhang, J. Liu, Y. Gao, M. Hua, B. Xia, P. Knecht, A. C. Papageorgiou, J. Reichert, J. V. Barth, H. Xu, L. Huang and N. Lin, Angew. Chem. Int. Ed., 2020, 59, 2669.

[2] M. N. Faraggi, C. Rogero, A. Arnau, M. Trelka, D. Écija, C. Isvoranu, J. Schnadt, C. Marti-Gastaldo, E. Coronado, J. M. Gallego, R. Otero, and R. Miranda, J. Phys. Chem. C, 2011, 115, 21177.

[3] R. González-Moreno, C. Sanchez-Sanchez, M. Trelka, R. Otero, A. Cossaro, A. Verdini, L. Floreano, M. Ruiz-Bermejo, A. García-Lekue, J. A. Martín-Gago and C. Rogero, J. Phys. Chem. C, 2011, 115, 6849.

[4] Q. Li, B. Yang, J. Björk, Q.G. Zhong, H. Ju, J.J. Zhang, N. Cao, Z.L. Shi, H.M. Zhang, D. Ebeling, A. Schirmeisen, J. F. Zhu and L. F. Chi, J. Am. Chem. Soc., 2018, 140, 6076.

[5] P. Giannozzi, et al., J. Phys.: Condens. Matter 2009, 21, 395502.

[6] L. A. Constantin, J. P. Perdew, J. M. Pitarke, Phys. Rev. B 2009, 79, 075126.

[7] J. P. Perdew, A. Ruzsinszky, G. I. Csonka, O. A. Vydrov, G. E. Scuseria, L. A. Constantin, X. Zhou, K. Burke, Phys. Rev. Lett. 2008, 100, 136406.

[8] G. Kresse, J. Joubert, Phys. Rev. B 1999, 59, 1758.

[9] J. D. Pack, H. J. Monkhorst, Phys. Rev. B 1977, 16, 1748

[10] S. Grimme, J. Antony, S. Ehrlich, H. Krieg, J. Chem. Phys. 2010, 132, 154104.

[11] M. Methfessel, A. T. Paxton, Phys. Rev. B 1989, 40, 3616.

[12] J. P. Lewis, P. Jelínek, J. Ortega, A. A. Demkov, D. G. Trabada, B. Haycock, H. Wang, G. Adams, J. K. Tomfohr, E. Abad, H. Wang, D.A. Drabold, Phys. Status Solidi Basic Res. 2011, 248, 1989–2007.

[13] F. J. Garcia-Vidal, J. Merino, R. Perez, R. Rincon, J. Ortega, Phys. Rev. B 1994, 50, 537–547.

[14] J. M. Blanco, F. Flores, R. Pérez, Prog. Surf. Sci. 2006, 81, 403–443.